

Associations between Sea Surface Temperature Gradient and Overlying Mid-Tropospheric Circulation in the North Pacific Region¹

ROBERT P. HARNACK AND ANTHONY J. BROCCOLI

*Department of Meteorology and Physical Oceanography, Cook College, Rutgers,
The State University of New Jersey, New Brunswick 08903*

(Manuscript received 28 March 1979, in final form 10 August 1979)

ABSTRACT

An attempt was made to verify and further investigate a proposed relationship between the location of the maximum east-west sea surface temperature anomaly gradient ($\Delta SSTA$) and the location of the maximum meridional component of the anomalous 700 mb geostrophic wind (V_gA) in the North Pacific on a monthly and seasonal time scale. Previous empirical studies, mostly of a case study type, had suggested collocation of maximum values of these variables in the same time period, particularly during the cold seasons. Using 31 years of monthly sea surface temperature and 700 mb height data for the North Pacific, the two variables were computed for each month and 3-month periods for each 10° longitude sector from $125^\circ W$ to $155^\circ E$, and for each of three latitude bands ($55\text{--}40^\circ N$, $40\text{--}25^\circ N$, $55\text{--}25^\circ N$). From these calculations, the spatial relationships of the two variables were determined by counting frequencies of the collocation of maximum V_gA and $\Delta SSTA$ for each month or season and latitude band, and by computing correlation coefficients between V_gA and $\Delta SSTA$ for each month or season and latitude band. Important seasonal and latitudinal differences were found for the strength of the relationship. It was concluded that the proposed relationship was best for the northernmost latitude band ($55\text{--}40^\circ N$), during winter and summer periods, and for 3-month means when compared to monthly means. Statistically significant relationships were found in several instances, indicating that the proposed relationship is probably a manifestation of real physical coupling between the ocean and atmosphere.

1. Introduction

There has been increasing interest in and study of large-scale air-sea interactions, with particular emphasis on the spatial relationship between the mean monthly or seasonal sea surface temperature anomaly (SSTA) distribution and mean monthly or seasonal atmospheric circulation. The primary motivation for this work is the eventual prediction of the state of one medium given that of the other, and then possibly using this knowledge to forecast mean surface temperature and precipitation. The physical reasons for expecting a linkage between mean sea surface temperature (SST) patterns and mean atmospheric circulation are that SSTA patterns often have much spatial coherence, cover large areas (i.e., 10^6 km^2), persist for several months (Namias and Born, 1974), and can be responsible for large sensible and latent heat fluxes from sea to atmosphere (Sawyer, 1965).

The question of whether an SSTA pattern leads an atmospheric circulation anomaly pattern, or vice versa, has still not been adequately resolved, as a reading of Davis (1976, 1978) would suggest. It

seems more accurate to think of the two media as being more or less coupled, with seasonally varying feedback mechanisms operating. This question of the ultimate causes of forcing will not be addressed here.

Of particular importance to atmospheric scientists involved in the short-range climate prediction problem, defined here as predictions on the monthly or seasonal time scale, is the relationship between anomalous atmospheric circulation and the concurrent or antecedent SSTA pattern. In a series of case studies, beginning with Namias (1959) and ending most recently with Namias (1978), that author has proposed and demonstrated significant and coherent spatial relationships between the two fields. He proposes that anomalous SST gradients produce and maintain enhanced atmospheric baroclinicity (through differential sensible and latent heat fluxes), which leads to anomalous cyclonic activity and anomalous mean sea level pressure and/or isobaric height distribution both locally and downstream. The purpose of many of these case studies was to demonstrate the relatively long-lived coupling (i.e., months or seasons) between the two media, as in Namias (1974), and to explore some of the possible causes for unusually persistent anomalous weather patterns (Namias, 1978). The arguments contained

¹ Paper of the Journal Series, New Jersey Agricultural Experiment Station, Cook College, Rutgers, The State University of New Jersey, New Brunswick.

in these works apparently have been convincing enough to warrant the use of sea surface temperatures in statistical prediction models such as those of Ratcliffe (1970), Harnack and Landsberg (1978), Harnack (1979) and Barnett and Preisendorfer (1978). These have shown that some degree of skill can be obtained when SST predictors are used. In addition, several numerical modeling experiments have been conducted using specified anomalous SST distributions (Houghton *et al.*, 1974; Kutzbach *et al.*, 1977; Huang, 1978) in order to assess the atmospheric response both locally and downstream. These studies have largely tended to confirm the ideas enunciated in the Namias works by showing significantly altered pressure distributions from those simulated using a normal SST distribution or using an SSTA distribution of opposite sign. However, the results have not been entirely conclusive. It should be borne in mind that most of the case studies and numerical simulations have been carried out for winter season conditions, when the energy flux from ocean to atmosphere is at a maximum, as is the expected atmospheric response. Furthermore, SSTA persistence is highest at this time due to the relatively large depth of the oceanic mixed layer (Namias and Born, 1974).

The purpose of the current study is to examine one proposed physical link, that between zonal SST gradients and overlying meridional tropospheric circulation, using the complete available climatic data base and extending the investigation to the non-winter months and seasons. By quantifying the apparent associations, the degree of reliability of predicting atmospheric circulation from SSTA patterns for all seasons can be more easily assessed. Furthermore, the nature of the physical association can be clarified.

One component of the well-known thermal wind relationship can be used to relate theoretically the zonal atmospheric temperature anomaly gradient in a layer to the meridional component of the anomalous geostrophic wind at the top of the layer (anomaly values refer to deviations from a long-term mean):

$$V_{g_2} - V_{g_1} = \frac{R}{f} \frac{\partial \bar{T}_a}{\partial x} \ln \frac{P_1}{P_2},$$

where

- V_{g_1} meridional component of the anomalous geostrophic wind at pressure level P_1
- V_{g_2} meridional component of the anomalous geostrophic wind at pressure level P_2
- \bar{T}_a integrated temperature anomaly of layer bounded by P_1 and P_2
- R gas constant for dry air
- f Coriolis parameter.

In order to relate observed frequency and degree of association between SST gradients and mid-tropospheric circulation to the theoretical ideas

expressed by the thermal wind equation, it must be assumed that anomalous SST gradients are associated with anomalous lower tropospheric temperature gradients in a layer and that the variation of mid-tropospheric circulation is primarily due to horizontal temperature gradient variations rather than to lower tropospheric circulation variations. Namias (1973) has attempted to answer the first question by correlating seasonal mean SST to 1000–700 mb thickness. He found that significantly large correlations are seen for large areas of the North Pacific in all seasons. These assumptions are certainly debatable but the purpose here was not to verify the validity of the thermal wind equation nor to use it for predictive purposes, but rather only to give the reader some theoretical rationale for explaining empirically determined associations between SST anomaly gradient and mid-tropospheric circulation. Applying these ideas to a possible zonal SST anomaly gradient/meridional 700 mb geostrophic wind relationship, as Namias (1978) has done in a case study sense, means that the location of the maximum southerly (northerly) component of the 700 mb anomalous geostrophic wind (V_gA) should coincide closely with the location of the maximum west-east (east-west) SST anomaly gradient ($\Delta SSTA$). Southerly component V_gA was defined with a positive sign, while northerly component V_gA was defined with a negative sign. For $\Delta SSTA$, SSTA increasing eastward was given a positive sign and SSTA decreasing eastward was given a negative sign.

The authors chose to investigate the relationship between *east-west* SST anomaly gradients and the *meridional* component of the anomalous geostrophic flow at 700 mb rather than the relationship between *north-south* SST anomaly gradients and the *zonal* component of the anomalous geostrophic flow at 700 mb because it is expected that the former type of relationships, if found to be significant, would be more useful for aiding the prediction of the amplitude and phase positions of tropospheric planetary-scale waves. The spatial relationship between these long-wave features and mean temperature or precipitation patterns has long been used by medium- and long-range forecasters (Namias, 1947; Klein, 1965). The authors recognize that the latter type of relationship also may have some importance, but it was felt that mixing the two ideas in one study might unduly tend to confuse what was considered to be the more important physical concept in the authors' opinion. Furthermore, the specific type of relationship investigated here is one that had already been invoked repeatedly in a case study sense, specifically in the references cited already, so that the time was right to attempt to validate the proposed relationship in an overall sense. The North Pacific Ocean region was selected for examining the spatial relationship between the two variables

since monthly and seasonal mean SST and 700 mb height data are readily available in usable form for this region, for an extended period, and because much attention has already been focused on the possible influence of Pacific large-scale air-sea interaction on short-term North American climatic anomalies.

2. Procedure

The following data were assembled for use in this study:

1) Mean monthly North Pacific SST on a 5° latitude, 10° longitude grid for the period 1947–77 in the area bounded by $25^\circ\text{--}55^\circ\text{N}$ and $125^\circ\text{W--}155^\circ\text{E}$ (Fig. 1). Missing data at some westernmost grid points in the high latitudes resulted in elimination of these areas from consideration in the analyses.

2) Mean monthly North Pacific 700 mb heights on a 10° latitude, 10° longitude grid for the period 1947–77 in the area bounded by $25^\circ\text{--}55^\circ\text{N}$ and $125^\circ\text{W--}155^\circ\text{E}$ (Fig. 1). These data were kindly provided on magnetic tape by the Scripps Institution on Oceanography.

For each month and season (all combinations of consecutive 3-month periods), a mean SST and 700 mb height field for the period 1947–76 was computed, then the SST anomaly and height anomaly values for each month and season in the sample were computed by subtracting the appropriate long-term monthly or seasonal mean value from the actual values. This procedure removes the possibility of strictly climatological relationships from being prominent in data analyses.

Next, for each month and season in the sample, east-west SST anomaly differences were computed at each latitude and for each 10° longitude sector, then for each longitude sector, three latitudinally averaged values were computed: 1) $40^\circ\text{--}55^\circ\text{N}$, 2) $25^\circ\text{--}40^\circ\text{N}$ and 3) $25^\circ\text{--}55^\circ\text{N}$. Due to missing data in the high latitudes, bands 1) and 3) had seven 10° longitude sectors, while band 2) had eight.

Similarly, for each month and season in the sample, the meridional component of the anomalous 700 mb geostrophic wind component (VgA) was computed from the sets of height anomalies for the same 10° longitude sectors and latitudinally averaged for the same latitude belts. The formula used in the calculation for each longitude sector and latitude is given as

$$VgA = \frac{g}{2\Omega \sin\phi} \frac{(ZA)_\lambda - (ZA)_{\lambda+10}}{a \cos\phi \Delta\lambda},$$

where ZA is the 700 mb height anomaly, λ the longitude, ϕ the latitude, a the radius of the earth, Ω the angular velocity of the earth and g the gravitational acceleration. Fig. 2 shows the grid points of 700 mb height anomalies used to calculate VgA for the northern latitude band for each longitude sector. A similar pattern of grid points was used for the other latitude bands. VgA was computed for each latitude involved, then all latitude values of VgA contained in each latitude band were averaged.

In order to more easily visualize the physical meaning of VgA and ΔSSTA for a given latitude band, Fig. 3 is presented, which is a schematic representation for a longitude sector.

The choice of 10° longitude spacing to define the sectors was of course arbitrary, but was selected in

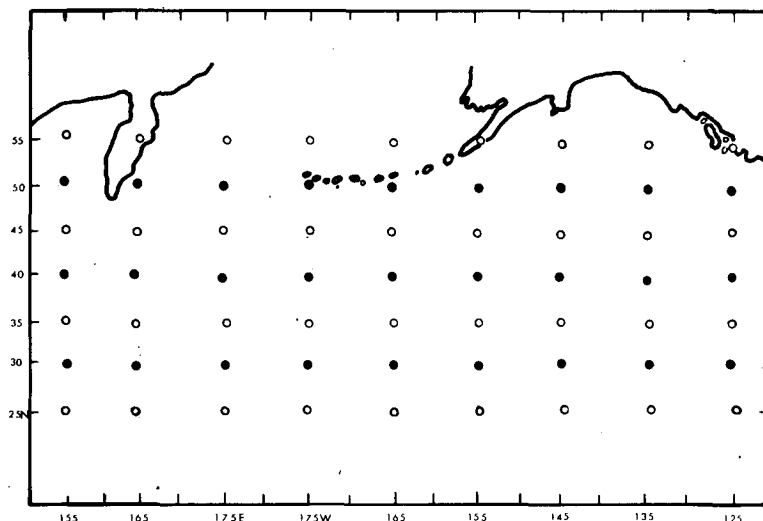


FIG. 1. Grid-point locations of 700 mb heights (open circles) and sea surface temperature anomalies (both open and closed circles) used in the study.

order to retain some detail in the SST anomaly gradient field and to still be consistent with the format and accuracy of the raw data used. The important thing here is that the same longitude spacing and latitudinal averaging was employed for both the SST anomaly and geostrophic wind computations.

From the sets of V_gA and $\Delta SSTA$ computed for each of the three latitude bands and for each month or season in the data sample, the particular longitude sector where the maximum positive and negative V_gA and the maximum positive and negative $\Delta SSTA$ occurred was determined. Each could occur in any one of seven or eight longitude sectors. From these determinations a contingency table was formulated for each month or season type, and for each latitude belt, which gave the frequency of having the maximum V_gA in each longitude sector, given the longitude sector of the maximum $\Delta SSTA$. These were produced for both southerly and northerly V_gA cases. If there is the kind of relationship expected from application of the thermal wind relationship, then there should be a relatively large number of cases in which the longitude sector of maximum V_gA is the same as or at least close to the longitude sector of maximum $\Delta SSTA$. Summing the number of cases on the diagonal of each contingency table yields a number that allows one to assess the overall degree of association between V_gA and $\Delta SSTA$, since this is the number of cases in which the southerly (northerly) V_gA and the positive (negative) $\Delta SSTA$ were collocated. Each table has a total of between 29 and 31 cases, corresponding to the number of usable years in the data sample for a given month or season type.

In addition, correlation coefficients were computed between all V_gA 's and $\Delta SSTA$'s for a given

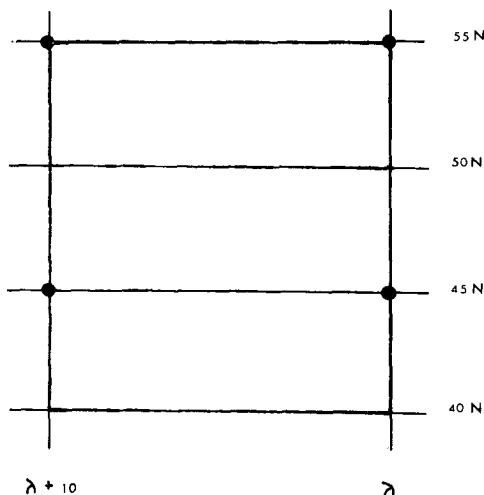


FIG. 2. An example of the latitude-longitude block used in the calculation of V_gA . Closed circles denote locations of 700 mb height anomalies used.

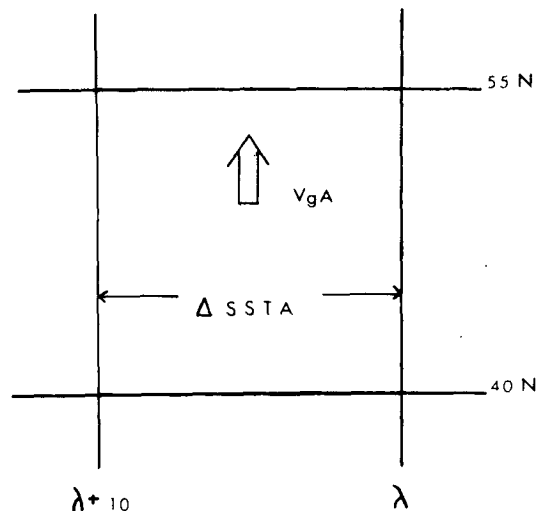


FIG. 3. Schematic example of the relationship between $\Delta SSTA$ and V_gA for a 10° longitude sector.

month or season type and latitude belt. These statistics further allow one to quantitatively assess the strength of the relationship.

3. Results and discussion

By summing along the diagonal of each contingency table, the number of cases when the longitude sector of maximum V_gA corresponds to the longitude sector of maximum $\Delta SSTA$ for each month/season and latitude belt was determined. Graphs were made for each latitude belt showing the number of cases when the longitude sector association of the type described actually occurred versus month or season type. These sets of graphs were produced for the relationship between southerly V_gA and positive $\Delta SSTA$ (i.e., SSTA increasing eastward) as well as between northerly V_gA and negative $\Delta SSTA$ (i.e., SSTA decreasing eastward).

Figs. 4 and 5 show the monthly variations by latitude belt of the frequency of collocation (i.e., diagonal sums) for southerly component V_gA /positive $\Delta SSTA$ and northerly component V_gA /negative $\Delta SSTA$, respectively. Totaling the diagonal frequencies over all months for each latitude band for the southerly component cases revealed that the $55\text{--}40^\circ\text{N}$ band had the most cases (99), compared with 82 cases for the $55\text{--}25^\circ\text{N}$ band. This means that for latitude band $55\text{--}40^\circ\text{N}$, 27% of all months in the data sample (370) had the maximum southerly component V_gA in the same longitude sector as the maximum positive $\Delta SSTA$. It should also be noted that 53% of all months had maximum southerly component V_gA within one 10° longitude sector of that for the maximum positive $\Delta SSTA$. For the northerly component V_gA situation, the latitude band $55\text{--}25^\circ\text{N}$ had the highest overall frequency,

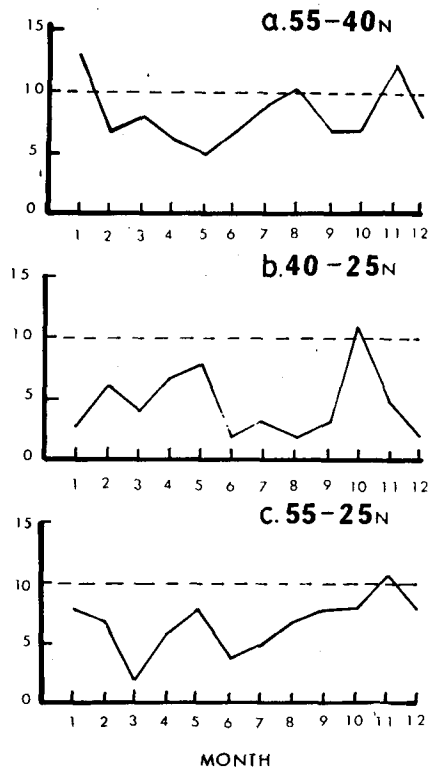


FIG. 4. Graph of the frequency of collocation of maximum positive Δ SSTA and maximum southerly VgA (ordinate) versus month type (abscissa) for (a) 55-40°N, (b) 40-25°N and (c) 55-25°N. Month 1 corresponds to January, month 2 to February, etc. Dashed lines denote the 5% significance level.

with 83 collocated (22%), while latitude band 55-40°N had a total of 72 cases (19%).

In order to assess the significance of the number of cases in which the maximum VgA was located in the same sector as the maximum Δ SSTA, a binomial test was used. For instances in which the sample size is sufficiently large (number of cases >25), it is possible to use the normal approximation to the binomial distribution. In the normal approximation, sample statistics (i.e., numbers of successes and failures) are compared with those expected by chance in terms of the Z statistic (Zar, 1974). The Z statistic is computed from

$$Z = \frac{|np - nc| - 0.5}{(npq)^{1/2}}, \quad (1)$$

where n is the number of cases, p the observed frequency of successes, q the observed frequency of failures and c the number of successes expected due to chance. By using the one-tailed critical value for the Z distribution corresponding to the appropriate significance level, it is possible to determine a critical value for the number of collocated maximum VgA and maximum Δ SSTA (i.e., cases along the diagonal) required to achieve significance

at the 5% level. For the northern latitude band, the probability of finding the maximum VgA and the maximum Δ SSTA to be collocated due to chance would be 1/7, so c would be set equal to 0.1429. A similar analysis can be performed to assess the significance of the occurrence of maximum VgA and maximum Δ SSTA within 10° of longitude of one another. Here, the probability of such an occurrence due to chance would be 19/49, so c would be set equal to 0.3878, and a critical value for significance at the 5% level can be determined in a similar manner. For individual months, each of which has between 29 and 31 cases, significance at the 5% level is achieved if 10 or more cases have collocated maximum VgA and maximum Δ SSTA, while for occurrence of maximum VgA within 10° of longitude of maximum Δ SSTA, 18 or more cases are required. Most of the discussion that follows relates to the analysis for the collocated situation.

Inspection of Fig. 4 reveals that well-defined summer and winter month maxima of frequency are seen for the 55-40°N band. For January, August and November the relationship was deemed significant at the 5% level. Nearly the reverse situation is seen for the 40-25°N band, but the frequencies are generally small and do not exceed chance expectation in a statistically significant way, except for the month of October.

For other combinations of latitude bands and component direction, the monthly variations are either

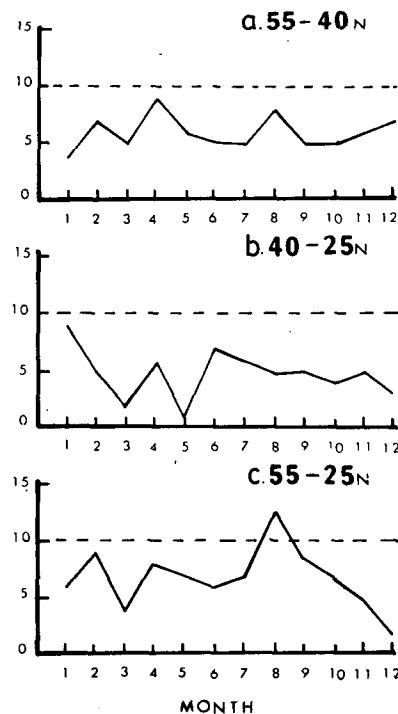


FIG. 5. As in Fig. 4 except ordinate is the frequency of collocation of maximum negative Δ SSTA and maximum northerly VgA.

quasi-random or the frequencies are relatively small or both. In particular, for northerly component VgA, only the relationship for 55–25°N for the month of August was deemed significant at the 5% level.

When comparing the overall total frequency for the southerly component VgA situation to the total frequency for the northerly component VgA situation, it was noted that significant differences occur only in the latitude band 55–40°N. In this comparison, 99 cases (27%) were counted for southerly VgA versus 72 cases (19%) for northerly VgA.

In summation, the proposed relationship between VgA and Δ SSTA on a monthly time scale is best for the northernmost latitude band (55–40°N) and for the southerly component VgA case. The relationship is statistically significant at the 5% level for three individual months.

Figs. 6 and 7 show the seasonal variation of the frequency of association between the longitude sector of maximum VgA and the longitude sector of maximum Δ SSTA for each of the three latitude belts. The first of these figures shows the situation for southerly component VgA, while the other figure shows the situation for northerly component VgA. Note that seasonal refers here to a 3-month mean, in which the months can be any consecutive 3 months. The plots have been made at the month type corresponding to the end month of the three months used in constructing the means.

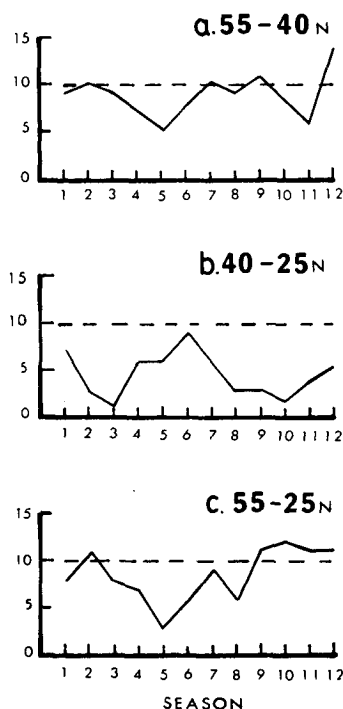


FIG. 6. As in Fig. 4 except abscissa is the season type, corresponding to a 3-month mean. Values are plotted at the end month of the three consecutive months used in calculating the mean.

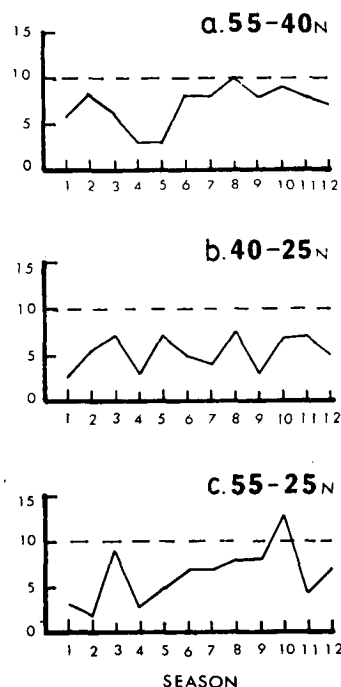


FIG. 7. As in Fig. 4 except abscissa is the season type and ordinate is the frequency of collocation of maximum negative Δ SSTA and maximum northerly VgA.

In comparing the overall seasonal to the monthly relationships, it is noted that the associations are generally better in the seasonal case, amounting to a 10–20% difference of number of cases when similar latitude belts are compared. Presumably, this is due to the increased time available for the atmospheric circulation and oceanic SST to adjust to one another, and particularly at the seasonal time scale, to the more dominant role large-scale air-sea interaction assumes in the Pacific region.

For both the southerly and northerly component VgA case, the overall percentage of seasonal cases having the proposed association was similar for latitude belts 55–40°N and 55–25°N, about 28% for southerly VgA and 22% for northerly VgA. However, for the lower latitude belt (40–25°N), the percentages drop to 15 and 18%, respectively. In general, for the seasonal portion of the study it found that the proposed spatial association between VgA and Δ SSTA was considerably stronger in the higher latitude band than in the lower latitude band. Perhaps this relates to the much higher frequency of cyclone passages in higher latitudes, which may be an integral part of the mechanism that links Δ SSTA to VgA.

In comparing the overall seasonal southerly VgA situation to the seasonal northerly VgA situation, it was evident that there were fewer cases of the proposed association for the northerly VgA situation. The reason for this is not clear.

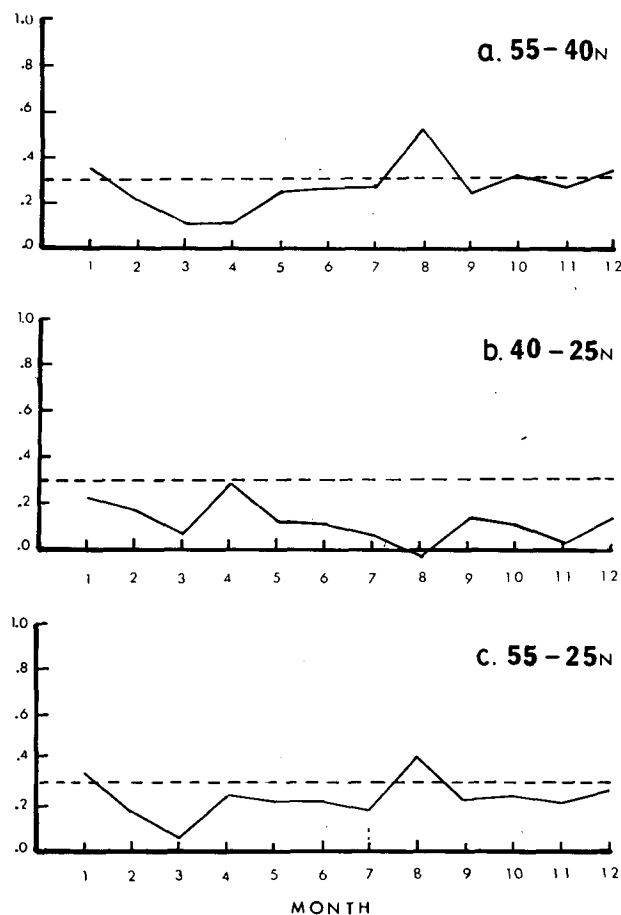


FIG. 8. Graph of the correlation coefficient computed between Δ SSTA and VgA versus month type for (a) 55-40°N, (b) 40-25°N and (c) 55-25°N. Dashed line denotes the 5% significance level.

In assessing the seasonal variation for the southerly VgA case in latitude band 55-40°N, a peak is seen for the October-December period (43%), a secondary peak is seen in the July-September period (40%), and minima occur for March-May (16%) and September-November (23%). Again, the expected percentage by chance is about 14%, so that the association is clearly nonrandom in the summer and late fall periods. Application of the binomial test showed statistical significance at the 5% level for the two maxima. For the northerly VgA case and other latitude bands, generally the number of collocations is small and, therefore, not worthy of a discussion about seasonal variation. The exception is the 55-25°N latitude band for the northerly VgA situation, where a major peak is seen for the August-October period (47%) and a minimum for the December-February period (13%). Again, the peak value was deemed to be significant at the 5% level.

The monthly and seasonal variation of the strength of the proposed relationship between VgA and Δ SSTA can be further assessed by inspection of

Figs. 8 and 9, which are plots of the overall correlation coefficient computed for each month or season type and latitude belt. The correlation coefficient was computed using all longitude sectors for each year, so that about 210 values for VgA and Δ SSTA were used in the computation. In order to determine statistical significance, only the individual years were considered to be independent cases. A standard *t*-test was used, assuming 28 degrees of freedom. A correlation coefficient exceeding 0.42 is required in this instance for statistical significance at the 1% level to be achieved. The 5% level value is 0.31.

For the monthly correlation coefficients, only August exceeded the 0.42 value, which occurred for latitude bands 55-40°N and 55-25°N. Several fall and winter months had correlation coefficients exceeding the 0.31 value, with most of these for the 55-40°N band.

For the seasonal correlation coefficients, the 3-month periods ending with each month from July through March had significant relationships in the latitude bands 55-40°N and 55-25°N. Many were significant at the 1% level. This means that only the

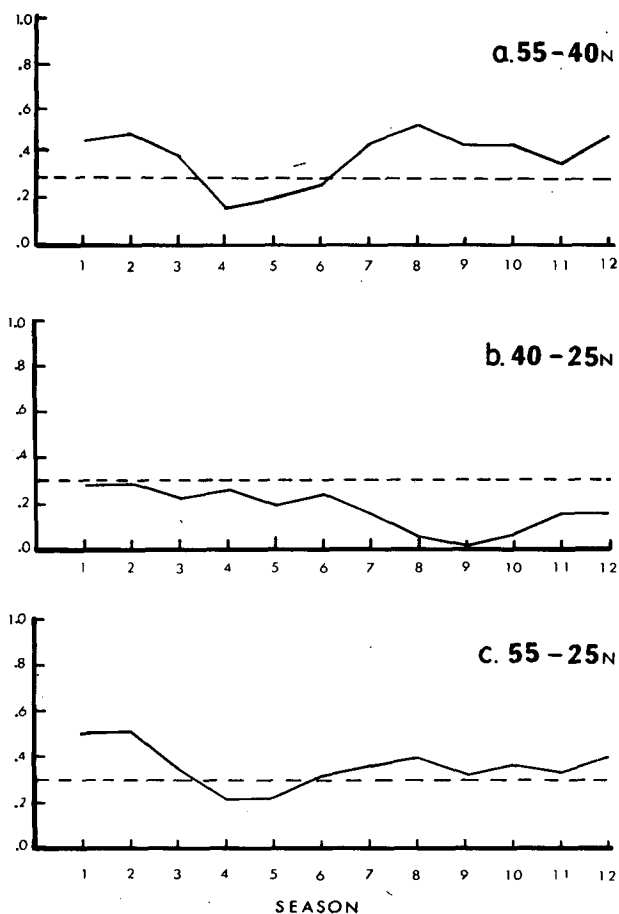


FIG. 9. As in Fig. 8 except abscissa is the season type. Plots were made at the end month of the three months used to define the seasonal mean.

spring season failed to have a statistically significant relationship in these latitude bands. No significant relationships were determined for the 40–25°N band. Clearly, as with the contingency table analysis, the relationship between VgA and Δ SSTA is much better in the more northerly latitudes.

In order for the reader to visualize the relationship between VgA and Δ SSTA for the individual cases, as well as to illustrate the range of observed relationships, Fig. 10 is presented which shows the longitude distribution of VgA and Δ SSTA in the latitude band 55–40°N for each standard summer season (June–August) in the sample (1947–77). Summer was selected for illustration since this season has been given less attention in the literature and since a surprisingly good relationship was found between the spatial distribution of VgA and Δ SSTA in this study. As one would expect from a sample of 31 years, there is a wide variety of patterns present, but by and large the spatial relationship between VgA and Δ SSTA can be characterized as good (i.e., an in-phase relationship) for much of the 1950's and early 1960's, especially in 1958 and 1964. However, a poor relationship is noted for 1959, 1962, 1963, 1965, 1968 and 1973. In other years the relationship is best described as fair.

This study finds that the proposed relationship, which first appeared in the literature in case studies for the winter season, is strongest overall in the summer season. This might possibly be important for successful summer circulation predictions, if forcing from ocean to atmosphere is important. Autocorrelations of SST for the May to summer season period, computed by the authors, are generally significant at the 1% level in the eastern Pacific region, so perhaps there is some inherent predictability in using the spring SSTA field for projecting summer season atmospheric circulation. A study by Davis (1978), however, did not find that spring SST could be used to predict summer sea level pressure with skill in the Pacific region. The results of the current study suggest that the entire matter needs further investigation, which is currently underway.

4. Summary and conclusions

An attempt was made to verify and further investigate a proposed relationship between the location of maximum east-west sea surface temperature anomaly gradient (Δ SSTA) and the location of the maximum meridional component of the anomalous 700 mb geostrophic wind (VgA) in the North Pacific on a monthly and seasonal time scale. A theoretical basis for an empirical finding of a collocation of maximum values of these variables in the same time period is the application of the thermal wind equation using anomalous components and assuming, among other things, that mean monthly or seasonal

sea surface temperature anomalies produce similar overlying atmospheric temperature anomalies. Previous empirical evidence of a proposed relationship was given most recently by Namias (1978), a case study of the 1976–77 winter season.

Using 31 years of monthly sea surface temperature and 700 mb height data for the North Pacific, the two variables were computed for each month and three monthly periods for each 10° longitude sector from 125°W to 155°E, and for each of three latitude bands (55–40°N, 40–25°N and 55–27°N). From these calculations, the spatial relationships of the two variables were determined by counting frequencies of the collocation of maximum VgA and Δ SSTA for each month or season and latitude band, and by computing correlation coefficients between VgA and Δ SSTA for each month or season and latitude band.

Analysis of these results led to the following principle conclusions:

- 1) The proposed relationships for southerly component VgA is best for the latitude band 55–40°N, when compared to 40–25°N or 55–25°N, although only slightly better than the latter.

- 2) The relationship is stronger for the location comparison of southerly component VgA to positive Δ SSTA (i.e., SSTA increasing eastward) than for the location comparison of northerly component VgA to negative Δ SSTA (i.e., SSTA decreasing eastward), especially for the 55–40°N band.

- 3) The summer and winter period relationships were generally stronger than those for the transition seasons, whether three monthly means or just monthly means were considered, for the southerly VgA cases in the latitude band 55–40°N. Statistically significant relationships were noted in many instances. It should be stressed that even the largest correlations are less than 0.6, so that much of the variance in the parameter calculated for one medium is unexplained by the variance in the parameter calculated for the other medium. Exceptions to the summer/winter peak of frequency or correlation were found for the other latitude band/VgA combinations, but in many cases statistical significance was not achieved. The proposed relationship was particularly poor for the spring months and season. This is not surprising given the rapid changes in both atmosphere and ocean that is occurring at this time of year, plus the fact that the oceanic response time to solar insolation changes is much slower than that of the atmosphere.

- 4) The proposed relationship was generally better for 3-month means than for monthly means, when the same latitude bands were being compared.

This study finds that anomalous meridional flow in the mid-troposphere is often associated with anomalous east-west sea surface temperature gradients in the North Pacific on a monthly and

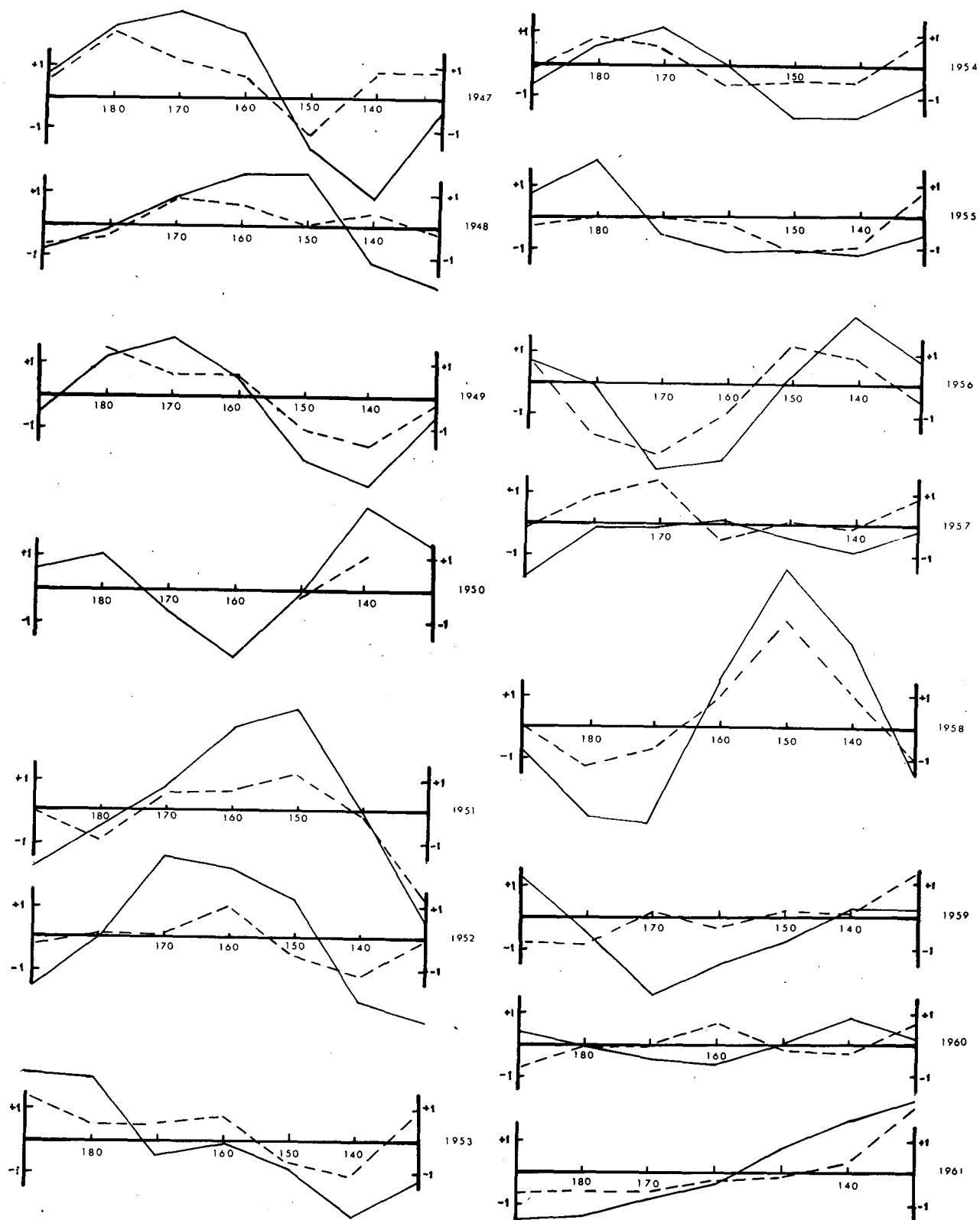


FIG. 10. Graphs of VgA (dashed) and SSTA (solid) versus longitude sector for each summer (June–August) in the period 1947–77. Units are m s^{-1} and $^{\circ}\text{C}$, respectively. Plots have been made at the midpoints of each 10° longitude sector.

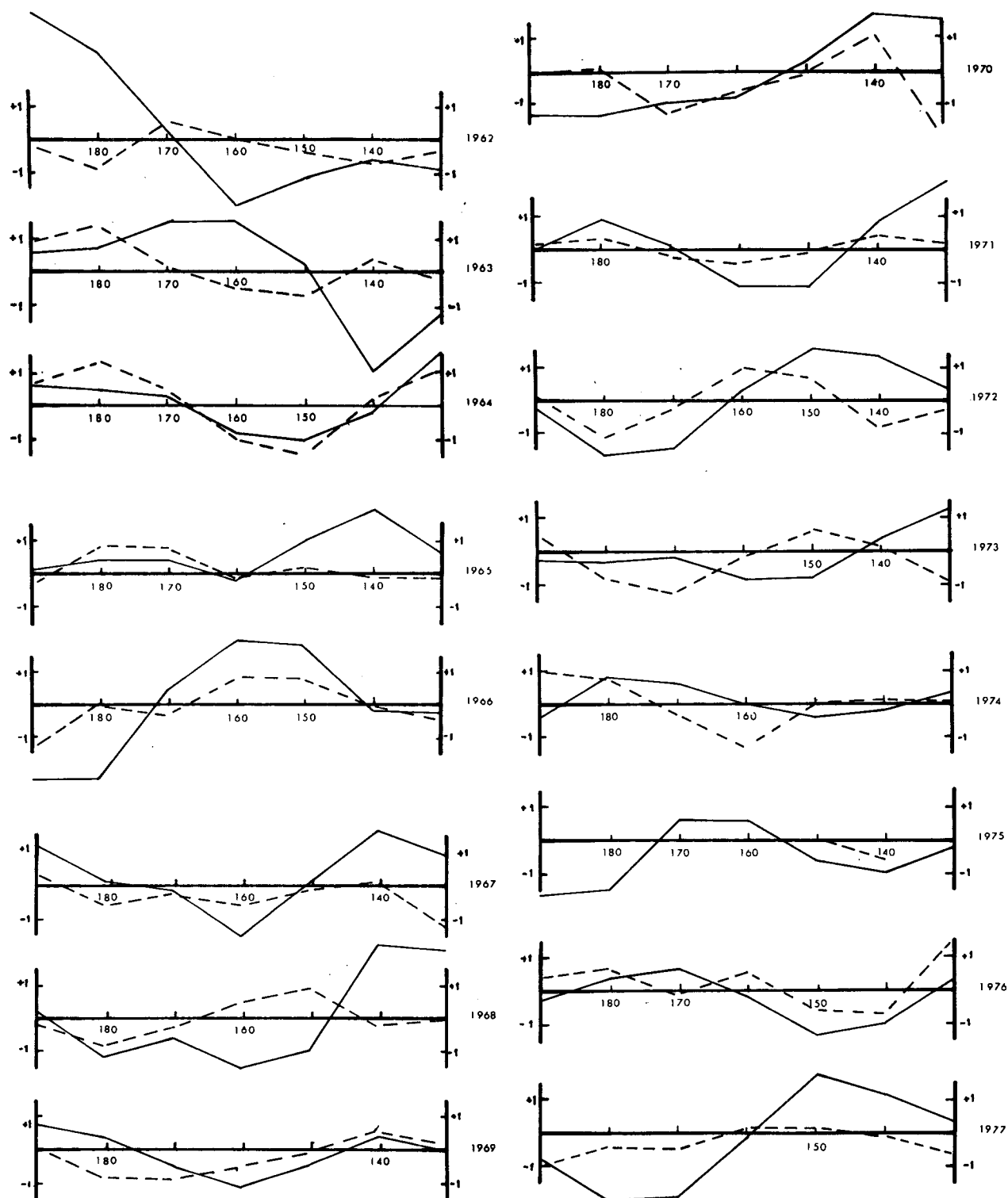


FIG. 10. (Continued)

seasonal time scale in the sense expected by application of the thermal wind equation and found in several individual cases in previous studies. Important seasonal and latitudinal differences were found for the strength of the relationship, which might possibly be useful information for the long-range forecasts of sea surface temperature anomalies or atmospheric circulation anomalies. In particular, a strong relationship is apparent in the summer season, which had not previously come to light. No attempt has been made to determine which medium, atmosphere or ocean, is forcing the other with regard to the variables considered here. Obviously, much additional work, both of an empirical and theoretical type, is needed to determine more about the nature of ocean-atmosphere coupling and interaction.

Acknowledgments. This research was supported by the Climate Dynamics Program, Division of Atmospheric Sciences, National Science Foundation, under Grant ATM-7815434, and by the New Jersey Agricultural Experiment Station under Project 276.

The authors wish to thank the following individuals for their assistance in the final completion of this study: Mr. Paul Schwartz for drafting the figures, Mr. Robert Born for supplying data from Scripps Institution of Oceanography, Mr. Edward Mandel for general assistance, Dr. William Swallow for statistical advice, and Mrs. Valeria Bowers for typing the manuscript.

Finally, suggestions made by the reviewers are most appreciated.

REFERENCES

- Barnett, J. P., and R. W. Preisendorfer, 1978: Multifield analog prediction of short-term climate fluctuations using a climate state vector. *J. Atmos. Sci.*, **35**, 1771–1787.
- Davis, R. E., 1976: Predictability of sea surface temperature and sea level pressure over the North Pacific Ocean. *J. Phys. Oceanogr.*, **6**, 249–266.
- , 1978: Predictability of sea level pressure anomalies over the North Pacific Ocean. *J. Phys. Oceanogr.*, **8**, 233–246.
- Harnack, R. P., 1979: A further assessment of winter temperature predictions using objective methods. *Mon. Wea. Rev.*, **107**, 250–267.
- , and H. E. Landsberg, 1978: Winter season temperature outlooks by objective methods. *J. Geophys. Res.*, **83**, 3601–3616.
- Houghton, D. D., J. E. Kutzbach, M. McClintock and D. Suchman, 1974: Response of a general circulation model to a sea temperature perturbation. *J. Atmos. Sci.*, **31**, 857–868.
- Huang, J. C., 1978: Response of the NCAR general circulation model to North Pacific sea surface temperature anomalies. *J. Atmos. Sci.*, **35**, 1164–1179.
- Klein, W. H., 1965: Application of synoptic climatology and short-range numerical prediction to five-day forecasting. Res. Pap. No. 46, U.S. Weather Bureau, Washington, DC, 109 pp.
- Kutzbach, J. E., R. M. Chervin and D. D. Houghton, 1977: Response of the NCAR general circulation model to prescribed changes in ocean surface temperature. Part I: Mid-latitude changes. *J. Atmos. Sci.*, **34**, 1200–1213.
- Namias, J., 1947: Extended forecasting by mean circulation methods. U.S. Weather Bureau, Washington, DC, 89 pp.
- , 1959: Recent seasonal interactions between North Pacific waters and the overlying atmosphere. *J. Geophys. Res.*, **64**, 631–646.
- , 1973: Thermal communication between sea surface and the lower troposphere. *J. Phys. Oceanogr.*, **3**, 373–378.
- , 1974: Longevity of a coupled air-sea-continent system. *Mon. Wea. Rev.*, **102**, 638–648.
- , 1978: Multiple causes of the North American abnormal winter 1976–77. *Mon. Wea. Rev.*, **106**, 279–295.
- , and R. M. Born, 1974: Further studies of temporal coherence in North Pacific sea surface temperatures. *J. Geophys. Res.*, **79**, 797–798.
- Ratcliffe, R. A. S., 1970: Sea temperature anomalies and long range forecasting. *Quart. J. Roy. Meteor. Soc.*, **96**, 337–338.
- Sawyer, J. S., 1965: Notes on the possible physical causes of long-term weather anomalies. Tech. Note No. 66, WMO, 227–237.
- Zar, J. H., 1974: *Biostatistical Analysis*. Prentice-Hall, 620 pp.